ELSEVIER

Superlattices and Microstructures 38 (2005) 168–183

Superlattices and Microstructures

www.elsevier.com/locate/superlattices

Acoustic phonon engineering in coated cylindrical nanowires

E.P. Pokatilov[1], D.L. Nika[1], A.A. Balandin*

Nano-Device Laboratory[2], Department of Electrical Engineering, University of California - Riverside, Riverside, CA 92521, USA

Received 22 April 2005; received in revised form 7 June 2005; accepted 7 June 2005
Available online 11 July 2005

Abstract

We have theoretically investigated the effect of a coating made of the elastically dissimilar material on the acoustic phonon properties of semiconductor nanowires. It is shown that the acoustic impedance mismatch at the interface between the nanowire and the barrier coating affects dramatically the phonon spectra and group velocities in the nanowires. Coatings made of materials with a small sound velocity lead to compression of the phonon energy spectrum and strong reduction of the phonon group velocities. The coatings made of materials with a high sound velocity have opposite effect. Our calculations reveal substantial re-distribution of the elastic deformations in coated nanowires, which results in modification of the phonon transport properties, and corresponding changes in thermal and electrical conduction. We argue that tuning of the coated nanowire material parameters and the barrier layer thickness can be used for engineering the transport properties in such nanostructures.

Keywords: Phonon engineering; Nanowire; Nanophononics; Phonon transport; Phonon confinement

* Corresponding author. Tel.: +1 909 787 2351; fax: +1 909 787 2425.
E-mail address: balandin@ee.ucr.edu (A.A. Balandin).

[1] On leave from the Department of Theoretical Physics, State University of Moldova, Kishinev, Republic of Moldova.

[2] http://ndl.ee.ucr.edu/.

0749-6036/$ - see front matter © 2005 Elsevier Ltd. All rights reserved.
doi:10.1016/j.spmi.2005.06.001

1. Introduction

Acoustic phonon spectrum modification in semiconductor superlattices and nanostructures continues to attract significant attention [1–7]. Folded acoustic phonons observed in superlattices [8] are described very well by the classical Rytov [9] model based on the elastic continuum approximation. The interest in the confinement-induced changes of the acoustic phonon dispersion in thin films and nanowires rose after it was suggested that they may lead to a reduction of the lattice thermal conductivity [10–12]. The modification of the acoustic phonon spectrum is particularly strong when the semiconductor structure size W becomes much smaller than the phonon mean free path Λ, i.e., $W \ll \Lambda$, and approaches the scale of the dominant phonon wavelength λ_d. For bulk Si, Λ is about 50–200 nm, while for many crystalline materials λ_d is on the order of 1.2–2 nm at room temperature, which approximately equals to the transistor gate dielectric thickness [13].

We have previously shown that the barrier layer made of elastically dissimilar material can strongly affect the acoustic phonon spectrum in planar three-layered heterostructures [14,15]. In that case, the total thickness of the heterostructure W_{tot}, which includes the core layer and two barriers, has to be much smaller than the phonon mean free path, $W_{\text{tot}} \ll \Lambda$, in order to modify the phonon spectrum. Pokatilov et al. [16] proposed that the redistribution of elastic vibration in planar heterostructure with acoustically soft barrier layers could lead to the phonon depletion in the acoustically hard core layer. We consider the material to be acoustically harder if it has larger acoustic impedance $Z = \rho V_S$ (V_S is the sound velocity and ρ is the mass density of the material). In this paper, we demonstrate that the phonon spectrum modification is much more pronounced in coated cylindrical nanowires than in planar heterostructures. Moreover, the acoustic phonon spectrum can be effectively tuned, i.e. engineered, by proper selection of the acoustically mismatched coating (barrier) layer parameters.

The remainder of the paper is organized as follows. Section 2 contains the derivation of the equation of motion for the elastic vibrations in the inhomogeneous cylindrical nanowire and the explanation of the calculation procedure. As an example material system we consider wurtzite GaN nanowires. High quality coated GaN nanowires have recently been fabricated and characterized [17]. Results of the calculation of phonon energy dispersion, phonon group velocity and the real-space distribution of the elastic energy are presented in Section 3. Our conclusions are given in Section 4.

2. Calculation procedure

As the material system of choice for our calculations we have selected wurtzite GaN due to its technological importance. High-quality coated GaN nanowires with radius as small as 5 nm and length up to several hundred micrometers have already been demonstrated [17]. Our theoretical model explicitly includes the specifics of the GaN hexagonal crystal lattice. In order to demonstrate the effect of the barrier shell coating on the phonon spectrum, we will consider GaN nanowire with the “acoustically fast” AlN and “acoustically slow” plastic barrier shell. Plastic coating is chosen for simplicity and to better elucidate the effect of phonon depletion. Our model calculations can certainly be extended to any other technologically more suitable material.

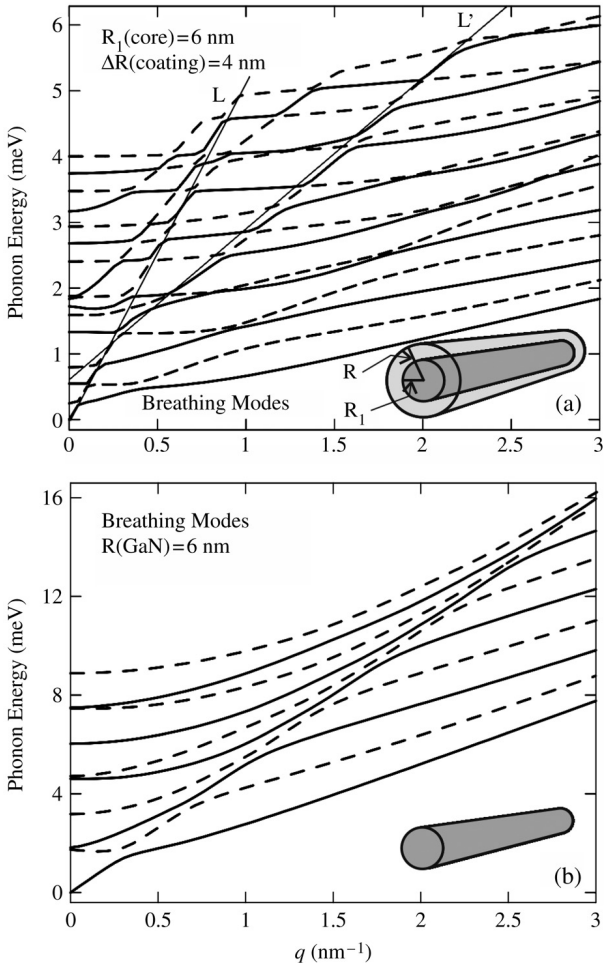

Fig. 1. Phonon energy as a function of the phonon wave vector q for the breathing modes ($m = 0$). The results are shown for (a) GaN nanowire with the "acoustically soft" barrier layer (R_1(GaN) $= 6$ nm and $R = 10$ nm); and (b) GaN nanowire without the barrier layer ($R = 6$ nm). The insets show the geometry of the nanostructures.

A schematic view of the considered structure is presented in the insets to Fig. 1. It is assumed that the axis c in wurtzite crystal is directed along the nanowire axis. To fully use the advantage of the cylindrical symmetry of structure, we use the cylindrical coordinate system with the radius vector $\vec{r}$ and angle φ in the cross-sectional plane, and axis Z along the nanowire axis. The radius of the nanowire core is designated as R_1 while the total radius of the hetero-nanowire (nanowire with the barrier layer) is designated as R. The thickness of the barrier shell (coating layer) is $\Delta R = R - R_1$. Both radii are assumed to be in the nanometer scale range to ensure the phonon confinement. The length of the nanowire is considered to be infinite. The phonon energy spectrum of the freestanding nanowire without coating is also calculated for comparison with the spectra of coated nanowires.

The equation of motion for elastic vibrations in an anisotropic medium can be written as [18]

$$\rho\frac{\partial^2 U_m}{\partial^2 t}=\frac{\partial\sigma_{mi}}{\partial x_i}, \tag{1}$$

where $\vec{U}=(U_1,U_2,U_3)$ is the displacement vector, ρ is the mass density of the material, σ_{mi} is the elastic stress tensor defined as $\sigma_{mi}=c_{mikj}U_{kj}$, and $U_{kj}=(1/2)((\partial U_k/\partial x_i)+(\partial U_i/\partial x_k))$ is the strain tensor. In the nanowire without the barrier shell, the elastic constants are $c_{iklm}=const$. In the cylindrical coordinate system, the displacement vector $\vec{U}$ has the following components: $U_r(r,\varphi,z)$, $U_\varphi(r,\varphi,z)$, $U_z(r,\varphi,z)$. Since the considered structure is homogeneous in the Z direction, we search for the solution of Eq. (1) in the following form

$$\begin{aligned}
U_r(r,\varphi,z)&=A(q)u_r(r)\cos m\varphi \mathrm{e}^{\mathbf{i}(\omega t-qz)}\\
U_\varphi(r,\varphi,z)&=A(q)u_\varphi(r)\sin m\varphi \mathrm{e}^{\mathbf{i}(\omega t-qz)}\\
U_z(r,\varphi,z)&=A(q)u_z(r)\cos m\varphi \mathrm{e}^{\mathbf{i}(\omega t-qz)},
\end{aligned} \tag{2}$$

where $m=0,\pm1,\pm2,\pm3,\ldots$. In Eq. (2), ω is the phonon frequency, q is the phonon wave vector, and $A(q)$ is the amplitude of a normal phonon mode and $\mathbf{i}$ is the imaginary unit. Performing the differentiation in Eq. (1) one needs to take into account that both the elastic moduli $c_{mikj}(r)$ and the mass density of the material $\rho(r)$ are piece-wise functions of r. For numerical simulation, the piece-wise functions are replaced with the smooth functions in such a way that their shape did not influence the results. We adopted the standard system of the two-index notations from Ref. [14]. In wurtzite crystals of hexagonal symmetry (space group C_{6v}^4), there are five different elastic moduli: c_{11}, c_{33}, c_{12}, c_{13} and c_{44}, which are related to each other through the following equalities $c_{11}=c_{1111}=c_{2222}$, $c_{33}=c_{3333}$, $c_{12}=c_{1122}=c_{2211}$, $c_{13}=c_{1133}=c_{3311}=c_{2233}=c_{3322}$, $c_{44}=c_{1313}=c_{3131}$, $c_{55}=c_{44}$, $c_{66}=c_{1212}=c_{2121}=\frac{c_{11}-c_{22}}{2}$.

Substituting Eq. (2) in Eq. (1), one can obtain the system of three equations for the three components of the displacement vector as

$$\begin{aligned}
(c_{44}q^2-\rho\omega^2)u_r&=c_{11}\frac{\mathrm{d}^2u_r}{\mathrm{d}r^2}+\left(\frac{c_{11}}{r}+\frac{\mathrm{d}c_{11}}{\mathrm{d}r}\right)\frac{\mathrm{d}u_r}{\mathrm{d}r}\\
&+\left(\frac{1}{r}\frac{\mathrm{d}c_{12}}{\mathrm{d}r}-\frac{c_{11}}{r^2}-\frac{m^2c_{66}}{r^2}\right)u_r+m\left(\frac{1}{r}\frac{\mathrm{d}c_{12}}{\mathrm{d}r}-\frac{c_{11}+c_{66}}{r^2}\right)u_\varphi\\
&+\frac{m(c_{11}-c_{66})}{r}\frac{\mathrm{d}u_\varphi}{\mathrm{d}r}+q(c_{13}+c_{44})\frac{\mathrm{d}u_z}{\mathrm{d}r}+q\frac{\mathrm{d}c_{13}}{\mathrm{d}r}u_z,\\
(c_{44}q^2-\rho\omega^2)u_\varphi&=c_{66}\frac{\mathrm{d}^2u_\varphi}{\mathrm{d}r^2}+\left(\frac{c_{66}}{r}+\frac{\mathrm{d}c_{66}}{\mathrm{d}r}\right)\frac{\mathrm{d}u_\varphi}{\mathrm{d}r}\\
&-\left(\frac{c_{66}}{r^2}+\frac{1}{r}\frac{\mathrm{d}c_{66}}{\mathrm{d}r}+\frac{c_{11}m^2}{r^2}\right)u_\varphi-\frac{m(c_{11}-c_{66})}{r}\frac{\mathrm{d}u_r}{\mathrm{d}r}\\
&-m\left(\frac{c_{11}+c_{66}}{r^2}+\frac{1}{r}\frac{\mathrm{d}c_{66}}{\mathrm{d}r}\right)u_r-\frac{mq(c_{13}+c_{44})}{r}u_z,
\end{aligned} \tag{3}$$

$$(c_{33}q^2-\rho\omega^2)u_z = c_{44}\frac{\mathrm{d}^2u_z}{\mathrm{d}r^2}+\left(\frac{c_{44}}{r}+\frac{\mathrm{d}c_{44}}{\mathrm{d}r}\right)\frac{\mathrm{d}u_z}{\mathrm{d}r}-\frac{c_{44}m^2}{r^2}u_z$$
$$-q\left(\frac{c_{13}+c_{44}}{r}+\frac{\mathrm{d}c_{44}}{\mathrm{d}r}\right)u_r-q(c_{13}+c_{44})\frac{\mathrm{d}u_r}{\mathrm{d}r}-\frac{qm(c_{13}+c_{44})}{r}u_\varphi.$$

In the case of the free-surface boundary conditions (FBC) on the outer surface of the nanowire, all components of the stress tensor are zero ($\sigma_{rr}=0$, $\sigma_{r\varphi}=0$ and $\sigma_{rz}=0$) for $r=R$, which leads to the following equations

$$\begin{aligned}&(c_{11}-c_{12})\frac{\mathrm{d}u_r}{\mathrm{d}r}+c_{12}\left(\frac{\mathrm{d}u_r}{\mathrm{d}r}+\frac{1}{r}u_r+\frac{m}{r}u_\varphi\right)+qc_{13}u_z=0,\\ &\frac{\mathrm{d}u_\varphi}{\mathrm{d}r}-\frac{m}{r}u_r-\frac{u_\varphi}{r}=0,\\ &\frac{\mathrm{d}u_z}{\mathrm{d}r}-qu_r=0.\end{aligned}\tag{4}$$

In the case of the clamped-surface boundary conditions (CBC) on the outer surface of the nanowire, all components of the displacement vector are zero ($u_r=0, u_\varphi=0, u_z=0$) for $r=R$.

The system of Eq. (3) has a solution for any integer value of m. At $m=0$, the system of three equations splits into subsystems of two equations for components u_r and u_z of the vector $\vec{u}=(u_r,u_z)$, and a separate equation for the $u_\varphi(r)$ function. The solutions of the system of two equations constitute the longitudinal-type "breathing" modes, which correspond to periodic dilatations and compressions of the cross-section of the nanowire. At $q=0$, the oscillations along the radius and the axis become independent and have different frequencies. The solution of Eq. (3) for u_φ describes the torsional oscillations around the nanowire axis. In these oscillations, the magnitude of the displacement vector is proportional to the radius and achieves its maximum on the nanowire surface. For $m\neq 0$, one needs to solve the system of the equations for all three components of the displacement vector. The solutions at $|m|=1$ are called the bending vibrations, while the solutions at $|m|>1$ are called the circular vibrations of $|m|$ order.

3. Results and discussion

The numerical calculations have been performed for the reference uncoated GaN nanowire with a radius $R=6$ nm and the coated GaN nanowire with the core radius $R_1=6$ nm. As a coating we considered different barrier shells such as "acoustical soft and slow" plastic with the thicknesses $\Delta R=4$ nm and $\Delta R=2$ nm, and "acoustically fast" AlN with the thickness $\Delta R=4$ nm. The material parameters for GaN and AlN required for our calculations have been taken from Ref. [19]. The chemical structure of the plastic material used as an example of the "acoustically slow" material is not essential for our elastic continuum analysis. We assume that the longitudinal sound velocity in bulk plastic is $V_L=2000$ m/s, transverse sound velocity is $V_T=1000$ m/s and the mass density is 1 g/cm^3 [14].

In Fig. 1(a) we present the breathing modes for GaN nanowire with the core radius $R_1=6$ nm embedded into the acoustically soft plastic shell with the thickness $\Delta R=4$ nm. The

total radius of the coated nanowire is $R = 10$ nm. The number S of the dispersion branches presented in Fig. 1(a) has been estimated from the relationship $S = R/2a$ (where a is the lattice constant). Assuming $a = 0.31$ nm, which is equal to the lattice constant of GaN in the plane perpendicular to the axis c, one gets $S \approx 16$. Each of the dispersion curves in the coated nanowire has narrow regions with distinctively different slopes. The steep segments of the dispersion curves reflect the properties of the "acoustically fast" material (GaN in this case). These segments can be approximated by a straight line, which is indicated in Fig. 1(a) by the symbol L. The slope of the straight line L is close to the sound velocity of the bulk transverse acoustic (TA) phonons in GaN. The slope of the straight line L' is close to the sound velocity of the bulk longitudinal acoustic (LA) phonons in the plastic material. It is interesting to note that the extent of the regions with the small slopes (in momentum space) is approximately one order of magnitude larger than the extent of the regions with the steep slopes although the cross-section area of "acoustically slow" material is only a factor of two larger than the cross-section area of the "acoustically fast" material. Another effect produced by the acoustically mismatched barrier layer is the compression of the confined phonon branches (increased number of branches per energy interval). The latter can be seen from the comparison of the spectrum in Fig. 1(a) with that of the nanowire without coating shown in Fig. 1(b). The breathing modes in uncoated GaN nanowire are calculated for the radius $R = 6$ nm, which is equal to the radius of the coated nanowire core in Fig. 1(a). In Fig. 1(a), there are 16 dispersion branches confined in the energy interval of 3.1 meV, while in Fig. 1(b) there are 10 branches in the wider energy interval of 9 meV.

Similar features can be seen in the spectra of torsional oscillations with $m = 0$. Fig. 2(a) shows torsional phonon modes in the nanowire with the core radius $R_1 = 6$ nm and the barrier shell thickness $\Delta R = 2$ nm. For comparison, Fig. 2(b) presents the torsional phonon modes for the uncoated GaN nanowire with the radius $R = 6$ nm. The dispersion of the torsional phonon modes in cylindrical nanowires resembles that of the shear phonon modes in thin films [14]. The torsional vibrations in the coated nanowire (which are also transverse) are hybridized. Their structure reflects the different acoustic properties of the nanowire core and the barrier shell. Fig. 3(a) shows the torsional phonon modes of the higher order ($m = \pm 2$) in the nanowire with the core radius $R_1 = 6$ nm and barrier shell thickness $\Delta R = 2$ nm. For comparison in Fig. 3(b), the same modes are presented for the nanowire without the barrier shell (coating). The amplitude of the oscillations for torsional modes periodically changes along the circumference while the directions of the vectors $u_\perp = (u_r, u_\varphi)$ are anti-parallel at the opposite ends of the nanowire diameter. Fig. 4(a) and (b) presents the dispersion curves for the bending oscillations ($m = \pm 1$ and $m = \pm 3$). The vectors $u_\perp = (u_r, u_\varphi)$ of these vibrations are parallel at the opposite ends of diameter. One can see that in all cases, the acoustically mismatched nanowire coating (barrier shell) introduces significant modification to the phonon spectrum. Moreover, different types of the phonon modes are sensitive to both the coating material and its thickness. The latter opens up a possibility of the phonon transport tuning in the acoustically mismatched nanowires by a proper selection of the barrier parameters.

The phonon group velocity dependence on frequency for different type of modes in the coated and uncoated nanowires is presented in Fig. 5(a)–(c). The phonon group velocities for the coated nanowires are shown within the range of energies where the predictions of the continuum approximation are unambiguous. For the convenience of comparison of

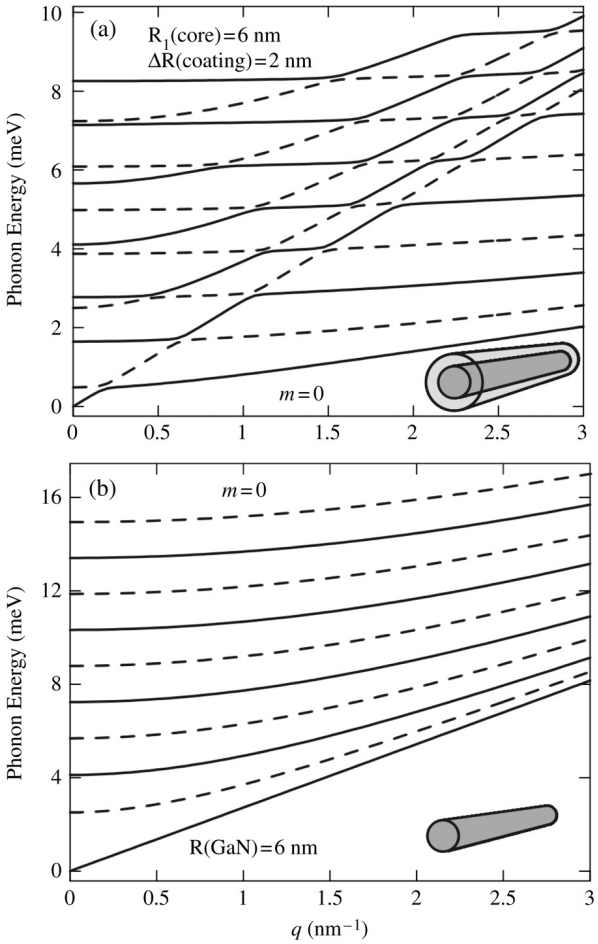

Fig. 2. The same as in Fig. 1 but for the torsional phonon modes with $m = 0$.

the phonon group velocity magnitudes, the average values of the velocities are shown in all figures by the straight horizontal lines. It follows from Fig. 5(a)–(c) that the average phonon group velocity for the breathing and bending waves in the GaN nanowire ($R_1 = 6$ nm) with the "acoustically slow" plastic coating ($\Delta R = 4$ nm) is three to four times smaller than that in the uncoated nanowire of the same radius in the examined energy range. One can see from Fig. 5(c) that the difference in velocities decreases with the reduction in the plastic shell thickness.

In Ref. [16] we defined the phonon depletion coefficient ξ and used this parameter to illustrate the redistribution of the lattice vibrations in the acoustically mismatched planar heterostructures. The magnitude of this coefficient characterizes the redistribution of the elastic energy between the "acoustically slow" and "acoustically fast" layers of a heterostructure. For a cylindrical nanowire, the phonon depletion coefficient, which is

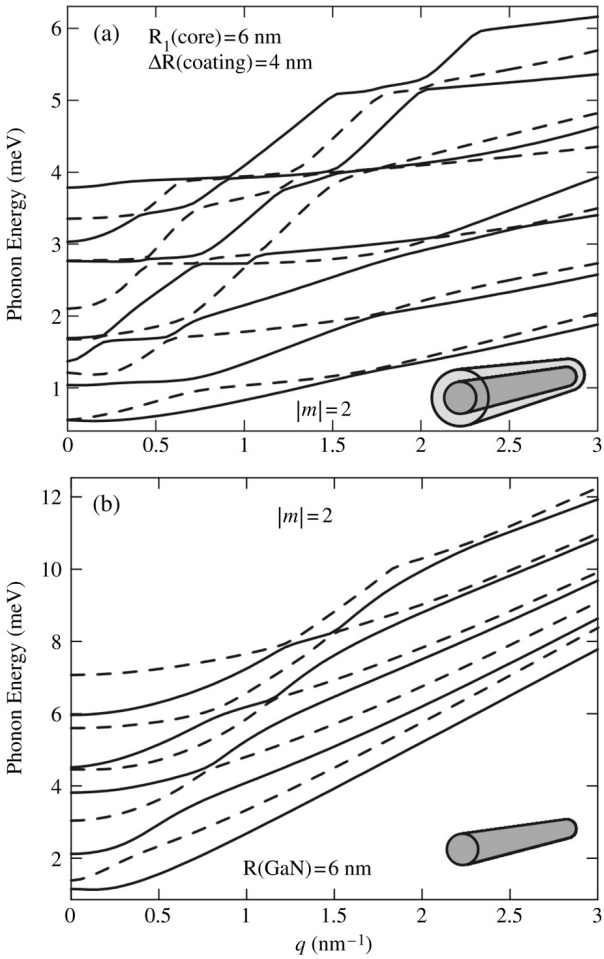

Fig. 3. The same as in Fig. 1 but for the torsional phonon modes with $|m| = 2$.

the ratio of the elastic energy inside the nanowire core to the elastic energy in the whole nanowire (both energies are taken per unit volume), is expressed by the formula

$$\xi_s^{(\alpha)}(q) = \frac{E_{s,1}(q)}{V_1}\frac{V}{E_s(q)} = \frac{R^2}{R_1^2}\frac{\rho_1 \int_0^{R_1} |\vec{u}_\alpha(r)|^2 r\,\mathrm{d}r}{\int_0^R \rho(r)|\vec{u}_\alpha(r)|^2 r\,\mathrm{d}r}, \tag{5}$$

where $V_1 = \pi R_1^2 L_z$, $V = \pi R^2 L_z$, $E_{s,1}(q)$ is the elastic energy in the nanowire core, $E_s(q)$ is the elastic energy in the whole nanowire, and index $s = 0, 1, 2, \ldots$ is the quantum number of a normal phonon mode.

In Fig. 6(a) and (b) we present the logarithm of the phonon depletion coefficients taken with the negative sign, $\zeta_s(q) = -\log \xi_s(q)$, as a function of the phonon wave vector q for the breathing and torsional modes ($m = 0$) in the coated nanowires with

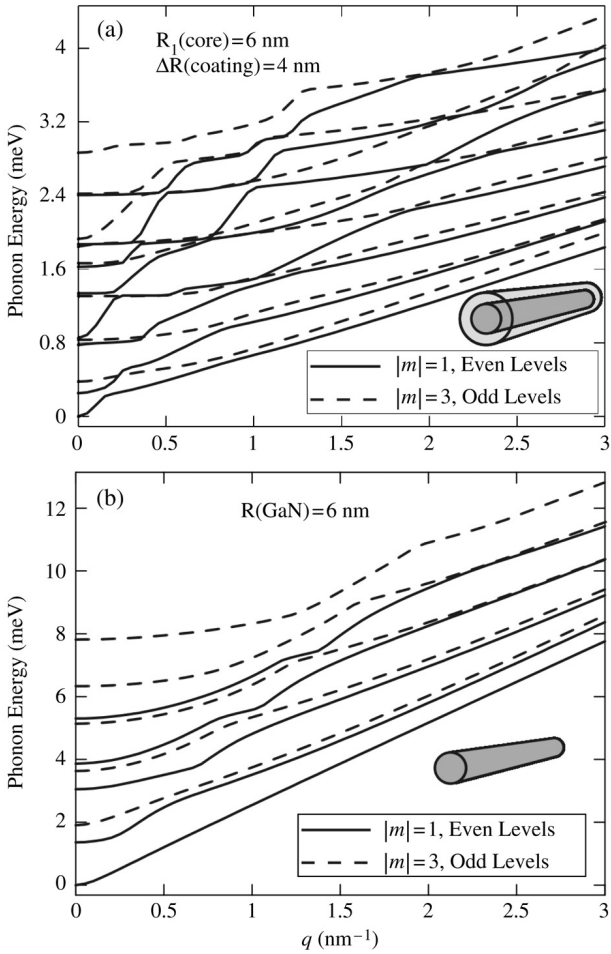

Fig. 4. Phonon energy as a function of the phonon wave vector q for torsional phonon modes (bending vibrations and circular vibrations of $|m| = 3$ order). The results are shown for (a) GaN nanowire with the "acoustically soft" barrier layer (R_1(GaN) $= 6$ nm and $R = 10$ nm); and (b) GaN nanowire without the barrier layer ($R = 6$ nm). Solid lines correspond to the even levels of the bending vibrations while the dashed lines correspond to the odd levels of circular vibrations of the $|m| = 3$ order.

$R_1 = 6$ nm and $\Delta R = 4$ nm. For the breathing modes the curves are qualitatively similar to those obtained in Ref. [16] for the planar heterostructures. At some value of the phonon wave vector q, the functions ζ_s reach a minimum, which is shifting in the direction of the larger q with an increase in the mode number. However, there is a considerable quantitative difference between the planar heterostructure and the nanowire cases. The values of $\zeta_s(q) \sim 4.0$ are reached in a cylindrical nanowire, which exceeds significantly the values $\zeta_s(q) \sim 1.5$–2.0 in the planar three-layered heterostructure of corresponding dimensions [16]. For the large values of the phonon wave vector $q \sim 2$ nm^{-1}, the phonon depletion coefficient in the considered nanowire achieves the value of $\zeta_s(q) \sim 5$. This

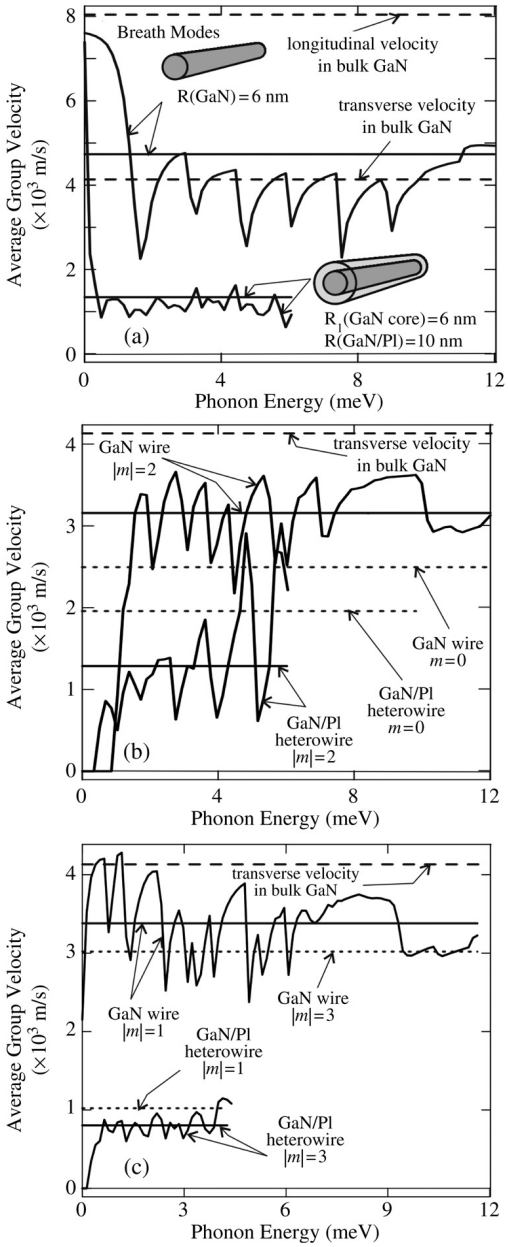

Fig. 5. Averaged phonon group velocity as a function of the phonon frequency for (a) breathing modes in the GaN nanowire with the "acoustically soft" barrier layer (R_1(GaN) = 6 nm, R = 10 nm) and the uncoated GaN nanowire (R = 6 nm); (b) torsional modes (m = 0 and $|m|$ = 2) in the GaN nanowire with the "acoustically soft" barrier layer (R_1(GaN) = 6 nm, R = 8 nm) and the uncoated GaN nanowire (R = 6 nm); (c) torsional bending modes (m = 1 and $|m|$ = 3) in the GaN nanowire with the "acoustically soft" barrier layer (R_1(GaN) = 6 nm, R = 10 nm) and the uncoated GaN nanowire (R = 6 nm).

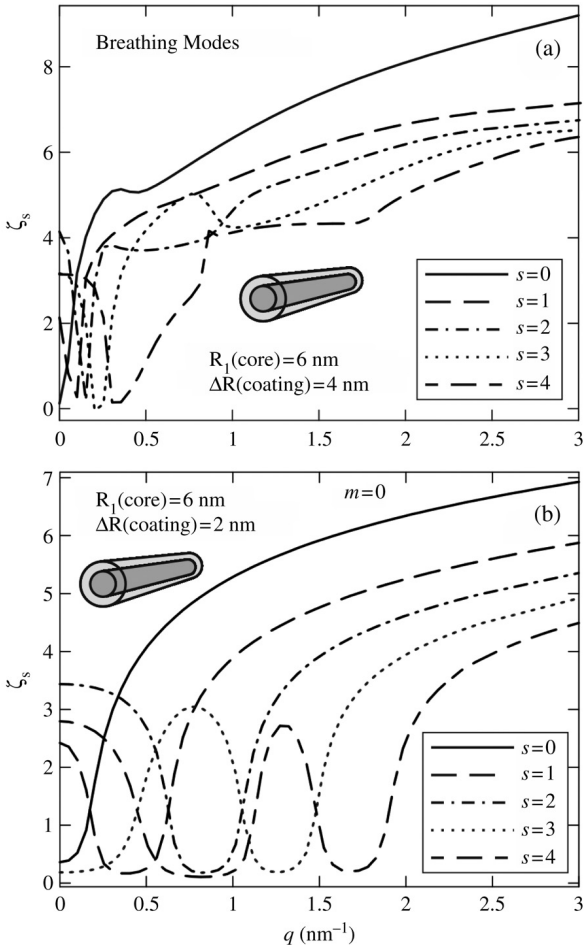

Fig. 6. Coefficient $\zeta_s(q) = -\log \xi_s^{(\alpha)}(q)$ as a function of the phonon wave vector q for (a) the breathing modes ($m = 0$) in the GaN nanowire with the "acoustically soft" barrier layer (R_1(GaN) $= 6$ nm, $R = 10$ nm); (b) torsional modes ($m = 0$) in the GaN nanowire with the "acoustically soft" barrier layer (R_1(GaN) $= 6$ nm, $R = 8$ nm).

means that the density of the vibration energy in the "acoustically slow" nanowire shell becomes five orders of magnitude larger than that in the "acoustically fast" GaN nanowire core. The bending vibrations ($|m| = 1$) and the circular vibrations ($|m| = 2, 3$) also demonstrate the giant value of the depletion coefficient (see Fig. 6(a) and (b) and Fig. 7(a) and (b)). The specific feature of the last example is that ζ_s remains very large at all values of the phonon wave vector q except for the narrow region around $q \sim 0.5$ nm^{-1} (for the modes with $s = 0, \ldots, 5$). Even in the nanowires with the relatively thin coating radius of $\Delta R = 2$ nm (see Fig. 7(b)), the phonon depletion coefficient remains very large, and exceeds corresponding coefficient values of planar heterostructures with the thick "acoustically slow" barriers [16].

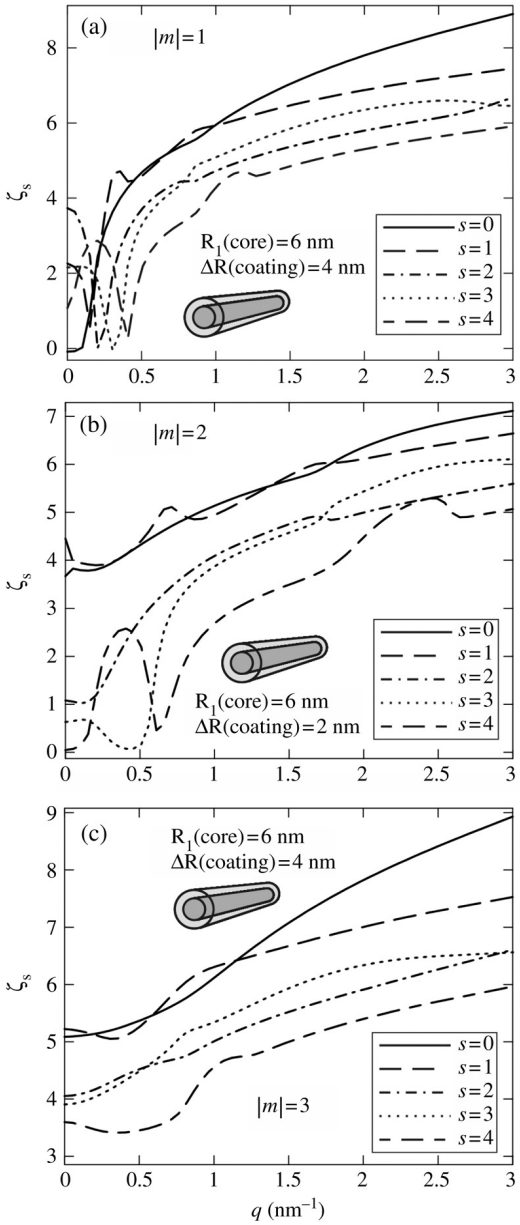

Fig. 7. Coefficient $\zeta_s(q) = -\log \xi_s^{(\alpha)}(q)$ as a function of the phonon wave vector q for (a) the torsional bending modes ($m = 1$) in the GaN nanowire with the "acoustically soft" barrier layer (R_1(GaN) = 6 nm, $R = 10$ nm); (b) torsional circular modes ($|m| = 2$) in the GaN nanowire with the "acoustically soft" barrier layer (R_1(GaN) = 6 nm, $R = 8$ nm); (c) torsional circular modes ($|m| = 3$) in the GaN nanowire with the "acoustically soft" barrier layer (R_1(GaN) = 6 nm, $R = 10$ nm).

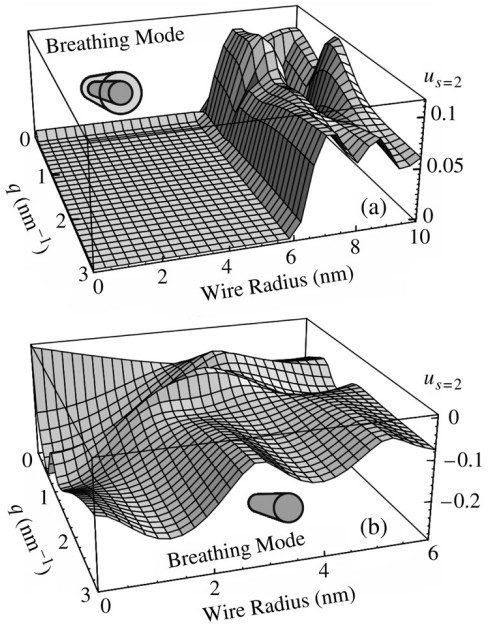

Fig. 8. Distribution of the displacement vector magnitude $u_{s=2} = \sqrt{u_r^2 + u_\varphi^3 + u_z^2}$ for breathing phonon mode with $s = 2$ in (a) the GaN nanowire with the "acoustically soft" barrier layer (R_1(GaN) = 6 nm, $R = 10$ nm); and (b) the GaN nanowire without the barrier layer ($R = 6$ nm).

To elucidate the physics of the phonon depletion in the acoustically mismatched nanostructures, we plot the re-distribution of the lattice displacements in coated nanowires (see Fig. 8(a) and (b), Fig. 9(a) and (b) and Fig. 10(a) and (b)). These figures show the surfaces formed by the displacement vector amplitude $u(r, q) = \sqrt{u_r^2(r, q) + u_\varphi^2(r, q) + u_z^2(r, q)}$ as the function of the real space coordinate r and the phonon wave vector q. As a reference, the distributions of the lattice displacements in the uncoated nanowires are also given. One can see from these figures a dramatic effect of the "acoustically slow and soft" barrier layers: the lattice vibrations, which are present in the uncoated nanowires, are almost completely pushed out of the "acoustically hard" nanowire core to the "acoustically soft" barrier. This re-distribution of the lattice displacements (vibration energy) explains the phonon depletion effect in the nanostructures with the acoustically mismatched barrier layers (coatings).

In order to evaluate the influence of the anisotropy of the wurtzite crystal lattice on the described processes we plot the phonon group velocity in GaN nanowire (core radius $R_1 = 6$ nm) with AlN barrier shell (the barrier thickness $\Delta R = 4$ nm) for the breathing modes with $s = 0$ and $s = 15$. For comparison, the phonon group velocity for the same modes calculated from the isotropic continuum approximation is also shown (see Fig. 11). One should note here that the anisotropy of the elastic moduli for given materials is relatively weak. For instance, in GaN $c_{11} = 390$ while $c_{33} = 398$ so that the anisotropy is around ∼2%. However, as follows from Fig. 11, the difference in the phonon group

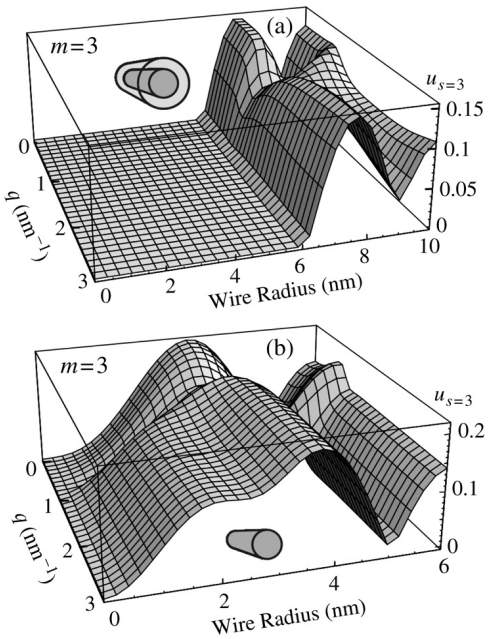

Fig. 9. Distribution of the displacement vector magnitude $u_{s=3} = \sqrt{u_r^2 + u_\varphi^3 + u_z^2}$ for the torsional circular phonon mode of the $m = 3$ order with $s = 3$ in (a) the GaN nanowire with the "acoustically soft" barrier layer (R_1(GaN) = 6 nm, $R = 10$ nm); and (b) the GaN nanowire without the barrier layer ($R = 6$ nm).

velocities for the isotropic and anisotropic cases for some values of the phonon wave vector q can be considerable.

In all considered examples of acoustic phonon engineering through the tuning of the barrier material parameters and thickness, we used the free-surface boundary conditions at the outer surface of the barrier shell. Qualitatively, the effects will be similar when the clamped-surface boundary conditions are used at the outer surface of the barrier shell. But, in the case of the clamped boundaries, confined phonon modes of all polarizations do not have a true bulk-type mode, i.e., $\hbar\omega_{s=0}(q = 0) \neq 0$. The effect of the clamped boundaries on phonon dispersion has been examined in details for thin films [2].

The choice of the free-surface boundary conditions for the external surface of the barrier shell is realistic due to the development of the Au nanoparticle — assisted metallorganic vapor phase epitaxy (MOVPE) growth of vertical nanowire arrays [20]. The parameters of the plastic used in our calculations roughly correspond to poly(N-vinyl-carbazole), which is used in light emitting technology [21]. The revealed modification of the acoustic phonon spectrum and group velocity in coated nanowires may affect the lattice (acoustic phonon) thermal conductivity through changes in the phonon density of states and the phonon scattering rates. For example, the acoustic phonon scattering rate on nanowire boundaries is given as $1/\tau_B \sim \langle V_G \rangle / D$, where $\langle V_G \rangle$ is the average phonon group velocity and D is the characteristic diameter of a nanowire.

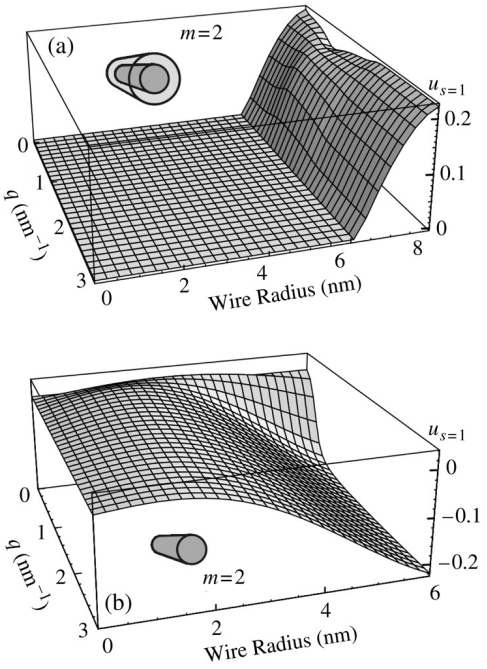

Fig. 10. Distribution of the displacement vector magnitude $u_{s=1} = \sqrt{u_r^2 + u_\varphi^3 + u_z^2}$ for the torsional circular phonon mode of the $m = 2$ order with $s = 1$ in (a) the GaN nanowire with the "acoustically soft" barrier layer (R_1(GaN) = 6 nm, $R = 8$ nm); and (b) the GaN nanowire without the barrier layer ($R = 6$ nm).

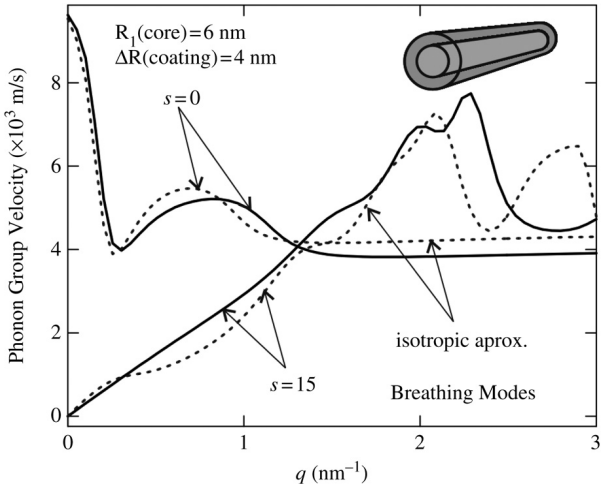

Fig. 11. Phonon group velocity as a function of the phonon wave vector q for breathing modes $s = 0$ and $s = 15$ in the GaN nanowire with the AlN barrier layer (R_1(GaN) = 6 nm, $R = 10$ nm). Solid lines correspond to the anisotropic case while the dotted lines correspond to the isotropic continuum approximation.

4. Conclusions

We have theoretically shown that the acoustic phonon properties in semiconductor nanowires can be engineered via proper selection of the acoustically mismatched barrier (coating) parameters. The barrier layers made of the materials with the small sound velocity lead to compression of the phonon energy spectrum and strong reduction of the phonon group velocities. The barrier layers made of the materials with the high sound velocity have an opposite effect. Our calculations show that the phonon depletion effect in the "acoustically hard" nanowire core embedded into an "acoustically soft and slow" barrier shell is much stronger in the cylindrical nanowire than in planar heterostructures. We argue that tuning of the coated nanowire material parameters and the coating thickness can be used for engineering the thermal and electrical properties of such nanostructures.

Acknowledgements

This work was supported in part through ONR award N00014-05-1-0150 to A.A.B. The authors thank Dr. V.A. Fonoberov for critical reading of the manuscript and providing useful comments. D.L.N.'s work was supported in part by CRDF-MRDA MTFP-04-06 for Young Scientists.

References

[1] V.G. Grigoryan, D.G. Sedrakyan, Akust. Zh. 29 (1983) 470.
[2] N. Bannov, V. Aristov et al., Phys. Rev. B 51 (1995) 9930.
[3] N. Nishiguchi, Y. Ando, M. Wybourne, J. Phys.: Condens. Matter 9 (1997) 5751.
[4] A. Svizhenko, A. Balandin et al., Phys. Rev. B 57 (1998) 4687.
[5] L.O. Lazarenkova, A.A. Balandin, Phys. Rev. B 66 (2002) 245319.
[6] S. Ruffo et al., J. Appl. Phys. 93 (2003) 2900.
[7] X. Lu, J.H. Chu, W.Z. Shen, J. Appl. Phys. 93 (2003) 1219.
[8] C. Colvard, T.A. Gant, M.V. Klein, R. Merlin, R. Fisher, H. Morkoc, A.C. Gossard, Phys. Rev. B 31 (1985) 2080.
[9] S.M. Rytov, Akust. Zh. 2 (1956) 71; Sov. Phys. – Acoust. 2 (1956) 67.
[10] A. Balandin, K.L. Wang, Phys. Rev. B 58 (1998) 1544; A. Balandin, K.L. Wang, J. Appl. Phys. 84 (1998) 6149.
[11] P. Hyldgaard, G.D. Mahan, Phys. Rev. B 56 (1997) 10754.
[12] J. Zou, A. Balandin, J. Appl. Phys. 89 (2001) 2932.
[13] A.A. Balandin, Thermal conductivity of semiconductor nanostructures, in: Encyclopedia of Nanoscience and Nanotechnology, ASP, Los Angeles, 2004, pp. 425–445.
[14] E.P. Pokatilov, D.L. Nika, A.A. Balandin, Superlatt. Microstruct. 33 (2003) 155; J. Appl. Phys. 95 (2004) 5625.
[15] A.A. Balandin, D.L. Nika, E.P. Pokatilov, Phys. Status Solidi (c) 1 (2004) 2658.
[16] E.P. Pokatilov, D.L. Nika, A.A. Balandin, Appl. Phys. Lett. 85 (2004) 825.
[17] J. Zhang, L. Zhang, F. Jiang, Y. Yang, J. Li, J. Phys. Chem. B 109 (2005) 151.
[18] L.D. Landau, E.M. Lifshits, Theory of Elasticity, Fizmatlit, Moscow, 2001.
[19] I. Vurgaftman, J.R. Meyer, L.R. Ram-Mohan, J. Appl. Phys. 89 (2001) 5815.
[20] K.A. Dick, K. Deppert, T. Martensson, B. Mandl, L. Samuelson, W. Seifert, Nano Lett. 5 (2005) 761.
[21] Y. Wenge et al., Displays 25 (2004) 61.